

Liquid/Gas Partition Coefficients of Aroma Compounds and *n*-Alkanes between Aqueous Ethanol Mixtures and Nitrogen

Albert L. Baner and Otto G. Piringer*

Fraunhofer-Institut ILV, Schragenhofstrasse 35, D-80992 Munich, Germany

Equilibrium liquid/gas partition coefficients between aqueous ethanol solutions and nitrogen were measured using a cocurrent gas/liquid equilibrium column for *n*-alkanes (pentane to hexadecane) and 13 different aroma compounds at very dilute concentrations. The operation of the column is described, and the results are compared to available literature results. The partition coefficients are compared to estimations made using the UNIFAC and GCFLORY (group-contribution Flory equation of state) activity coefficient estimation models. The estimations are generally accurate within an order of magnitude, with some exceptions.

Introduction

Equilibrium partitioning of aroma compounds between foods and their package headspace plays an important role in migration and food quality considerations in food/package systems. Essential data required are vapor/liquid equilibrium (VLE) data for aroma compounds at room temperature (22–27 °C). Aroma compounds are largely unsaturated oxygen-containing compounds having complex molecular structures with molecular weights ranging from 100 to 300. These compounds tend to have very low volatilities at room temperature (pure component vapor pressures <1.3 kPa) and are mostly present in foods in dilute concentrations ($x_i \leq 1 \times 10^{-4}$).

Pure component properties such as vapor pressure (especially at room temperature), critical temperatures and pressures, dipole moments, densities (some aromas are solid at room temperature), etc. are often not available and thus effectively prevent the use of most correlative estimation methods as well as effective use of vapor-phase corrections needed for many VLE measurement methods. Other VLE estimation methods such as the various group-contribution methods are semiempirical in nature and are based on VLE data of low molecular weight solvent compounds with simple structures which results in estimations of aroma properties with a high degree of uncertainty. Furthermore, foods and food matrices are very complex and labile mixtures, so from practical and analytical considerations it is necessary to use food simulants to model VLE behavior in food systems (1–3). The goal of this work was to measure partition coefficient VLE data for aromas with low volatilities between relatively volatile ethanol and aqueous ethanol mixtures and nitrogen at 25 °C.

The lack of accurate pure component vapor pressures for aromas effectively limits accurate VLE measurements to equilibrium partition coefficients since the pure vapor pressures (standard-state fugacity) are needed to determine activity coefficients for some alternative experimental methods. Methods such as ebulliometry (4) and distillation (5) cannot use ethanol and ethanol/water solvent systems at 25 °C. Headspace gas chromatography (6) suffers from insensitivity to involatile compounds, and inert gas stripping (also exponential dilutor method) (7) has not been used for solvent mixtures and may suffer from changes in the solvent phase during the stripping process. Gas chromatographic (GC) retention time methods (8, 9) require that the solute be more volatile than the solvent which eliminates these types of methods from consideration.

At 25 °C and atmospheric pressure there are effectively two types of approaches for direct determination of aroma compound equilibrium partition coefficient data between liquids and gases. One is a kinetic method based on the rate of loss of a substance from liquid by stripping with an inert gas (gas purge method) (10). The other is a thermodynamic method where the air and water concentrations are measured and the partition coefficients are calculated as their ratio (11). Recently GC equilibrium headspace methods have been reported (12, 13) whereby only headspace concentrations need to be determined.

The advantages of the kinetic method are the relatively small vessel volumes in gas–water contact and consequently small adsorption areas and equilibrium times. A disadvantage of the kinetic method lies in the need of a model. All models are approximations, and the use of mass-transfer coefficients for the evaluation of thermodynamic partition coefficients is a principal disadvantage. A consequence of using such approximations is the possibility of introducing systematic errors of unpredictable magnitudes.

The advantage of the static, thermodynamic method is the direct determination of the equilibrium concentrations in the two phases. The disadvantage is the long equilibrium time for a large gas volume with a large gas to vessel interface and the associated adsorption phenomena, as well as the need for very careful handling of the gas sample for analysis so that the gas/liquid equilibrium is not disturbed.

In order to combine the advantages and avoid the disadvantages of the above two approaches, a dynamic method using a column operating in cocurrent mode that produces a guaranteed phase equilibrium was used. In this paper, the apparatus and its mode of operation are described and equilibrium partition coefficients for 13 aromas and *n*-alkanes from pentane to hexadecane partitioned between ethanol and aqueous ethanol mixtures at 25 °C are reported. The equilibrium partition coefficients are then compared with values estimated by the UNIFAC and group-contribution Flory equation of state (GCFLORY) group-contribution activity coefficient estimation models.

Apparatus and Procedure

Liquid/air partition coefficients were measured using cocurrent flows of liquid and air (nitrogen) in a thermostated gas/liquid equilibrium column (Normag GmbH, Hofheim/Taunus, Germany). The column itself has been previously used (14, 15). Figure 1 shows a scheme of the column system used. This continuous-flow method under steady-state operation conditions uses very large liquid and gas volumes

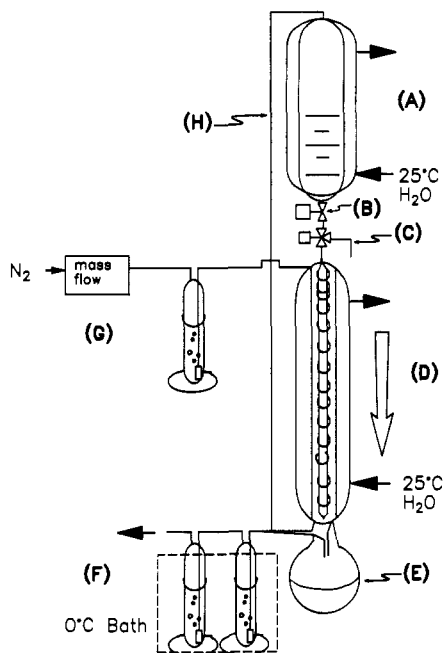


Figure 1. Schematic diagram of the gas/liquid equilibrium column apparatus.

so that errors due to adsorption on the surfaces of the apparatus are negligible. The column has a thermostated 2-L upper reservoir (A), a metering valve for controlling the liquid flow rate (B), a sample valve for removing liquid samples from the upper reservoir (C), and a thermostated gas stripping column (D) that allows for long contact times between a thin film of liquid flowing along a glass spiral wound on a thermostated inner tube and a cocurrent flow of nitrogen. The geometry of the glass helix ensures sufficient contact time for the establishment of partition equilibrium. The column has an effective spiral length of 62 cm, an inner diameter of 1.5 cm, an outer diameter of 3.0 cm, and a total length of 115 cm. At a flow rate of $130 \text{ cm}^3 \cdot \text{h}^{-1}$ a drop of water requires 250 s to travel through the column. At the bottom of the column the liquid flows through a capillary tube, which serves to separate the gas and liquid phases, and then into a collecting reservoir (E). The saturated nitrogen stream then passes through two gas washing bottles in series with no. 2 pore frits containing ethanol held at 0°C using a polyethylene glycol bath (F).

The column temperature was held at $25 \pm 0.5^\circ \text{C}$ using two Lauda RCS6 (Messgeräte-Werk Lauda GmbH, Lauda-Königshofen, Germany) circulating water baths with R22 remote temperature controllers and Pt(100) thermal resistance temperature sensors for controlling temperature. The actual temperature at the end of the column was measured with a Pt(100) temperature sensor and recorded on a strip chart recorder. The incoming nitrogen stream was conditioned at 25°C by flowing it through a coil in the water bath. The flow rate was controlled to within $\pm 1 \text{ cm}^3 \cdot \text{min}^{-1}$ using a MKS Instruments (Munich, Germany) Model 1259C 500 cm^3 mass flow controller with a MKS PR-3000 controller which had an accuracy of 0.8% of full scale and a resolution of 0.1% of full scale. The nitrogen stream was saturated with ethanol and water vapor (depending on the liquid phase being measured) by passing it through a gas washing bottle containing the liquid-phase solvent with a no. 2 frit (G) prior to entering the column. The nitrogen flow at the end of the column was remeasured using a soap bubble flow meter. Additional temperature control was provided by heating tapes and strings (Horst Laborgeräte GmbH, Lindfels-Seidenbuch, Germany) connected to Normag digital proportional tem-

perature controllers with Pt(100) sensors at the liquid sampling valve (B), the nitrogen conditioner (G), and the gas outlet at the end of the column.

It is important when the column is operating at temperatures above room temperature that the liquid from the water bath flows first through the outer jacket of the column and then into the inner tube to prevent condensation on the outer column wall. To overcome the slight back-pressure created by the two gas washing bottles at the end of the column, a pressure-equalizing tube was connected between the bottom of the column and the top of the reservoir (H). This helped to maintain a constant flow of liquid throughout the course of a measurement.

A measurement was begun by filling the upper reservoir with a measured volume of liquid solvent containing a mixture of solutes and allowing it to equilibrate for 30 min. The liquid mixture contained a mixture of 13 aromas each having a mole fraction of 7.7×10^{-6} (total solute mole fraction 1×10^{-4}) which corresponds to individual aroma concentrations of 12–24 ppm ($\mu\text{g} \cdot \text{cm}^{-3}$). The *n*-alkanes were measured using a mixture of 9 *n*-alkanes having mole fractions of 1×10^{-4} for ethanol, 3.0×10^{-7} to 4.0×10^{-5} for $w_i = 0.66$ aqueous ethanol and 7.0×10^{-8} to 1.9×10^{-5} for $0.33 w_i =$ aqueous ethanol corresponding to 129–392, 1.8–84, and 0.77–58 ppm.

Prior to beginning a measurement, the system was pre-conditioned by flowing the gas and liquid streams under experimental conditions for 1 h. This is done to ensure the column reaches equilibrium as soon as possible after starting a measurement. After the conditioning period, the gas and liquid flows were temporarily halted, a sample was taken from the upper reservoir and collection flask (E), and gas washing bottles (F) were changed. The liquid flow was then re-established and the experiment begun with the flow of gas through the column. After 12–14 h (overnight) the experiment was complete and the volumes of liquid in the upper reservoir, collection flask, and gas washing bottles were measured. Samples for GC analysis were taken from the upper reservoir, the collection flask, and the two gas washing bottles. The liquid/gas partition coefficient, $K_{L/G}$, defined as the ratio of the concentration of solute in the liquid phase ($\text{g} \cdot \text{cm}^{-3}$) to the concentration in the gas phase ($\text{g} \cdot \text{cm}^{-3}$) was calculated using eq 1, where au are the GC area units for a partitioned substance,

$$K_{L/G} = \frac{(au_L)tv_G(\text{cal}_L)}{((au_{G,1})V_{G,1} + (au_{G,2})V_{G,2})(\text{cal}_G)} \quad (1)$$

V is the volume (cm^3) at the end of a run, t is the time (s), v ($\text{cm}^3 \cdot \text{s}^{-1}$) is the volumetric flow of the gas, and cal is the GC calibration factor ($\text{g} \cdot \text{cm}^{-3} \cdot \text{au}^{-1}$) for the respective phases. The subscripts L, G, 1, and 2 stand for liquid, gas, and gas washing bottles 1 and 2, respectively. A percent recovery was calculated using eq 2, where the subscripts UO and UE stand

$$\% \text{ recovery} = 100 \left[\frac{((\text{cal}_L)((au_{UE})V_{UE} + (au_L)V_L) + (\text{cal}_G)((au_{G,1})V_{G,1} + (au_{G,2})V_{G,2}))}{(\text{cal}_L)(au_{UO})V_{UO}} \right] \quad (2)$$

for the upper reservoir concentration at the beginning and end of a measurement.

The liquid/gas partition coefficient can also be calculated using the concentration difference between the upper reservoir and the lower reservoir provided a significant difference between the upper and lower reservoir concentrations can be measured:

$$K_{L/G} = \frac{(au_L)tv_G}{[(au_{UE} + au_{UO})/2] - au_L} \quad (3)$$

The initial column operating parameters were taken from

Table 1. Purities of Test Compounds

aroma compd	purity (mass %)	<i>n</i> -alkane	purity (mass %)
D-limonene	94.2	pentane	>99
diphenylmethane	94.2	hexane	>99
linalyl acetate	91.8	heptane	>99
camphor	94.1	octane	>99
diphenyl oxide	99.9	nonane	>99
isoamyl acetate	98.0	decane	>98
γ -undelactone	98.0	dodecane	>98
eugenol	98.6	tetradecane	>99
citronellol	96.2	hexadecane	>98
dimethylbenzylcarbinol	99.6		
L-menthol	99.2		
phenylethyl alcohol	99.7		
<i>cis</i> -3-hexenol	94.1		

previous work with this column (14, 15). The optimal operating nitrogen gas flow rates for these traps were evaluated using a mixture of *n*-alkanes (pentane to dodecane) in ethanol with a liquid flow rate of 1–3 cm³·min⁻¹ over 12–15 h and determined to be 100–300 cm³·min⁻¹, taken as the minimum of a curve of $K_{L/G}$ plotted versus the gas flow rate.

It was found that $K_{L/G}$ calculated using concentration differences (eq 3) worked only for the more volatile solutes and is best used as a control to check the $K_{L/G}$ calculated using the solvent trap (eq 1). Solute with low volatilities show practically no measurable concentration change in the liquid phase. If the concentration difference $K_{L/G}$ is smaller than the solvent trap $K_{L/G}$, then the trap is not retaining all of the substance from the gas phase.

The effect of solute concentration in the liquid phase was tested by increasing the concentration of the aroma mixture in a $w_i = 0.50$ aqueous ethanol solution 20 times (from ~20 ppm ($\mu\text{g}\cdot\text{cm}^{-3}$) to ~244 ppm). The result was such that within the method's experimental uncertainty no significant difference at $\alpha = 0.05$ was seen between the measured partition coefficients.

Materials

Ethanol (purity >99.8% mass %) from Merck (Darmstadt, Germany) and deionized laboratory water were used to make up the liquid phase. Nitrogen (99.9999% pure) (purity 5.0, GC grade) from Linde (Munich, Germany) was used.

Aromas were supplied by Drom Parfümöle KG (Baierbrunn, Germany), and the *n*-alkanes were from Fluka Chemie (Buchs, Switzerland). The purities of the aromas determined by GC are given in Table 1 together with the purities of the *n*-alkanes which were used as purchased.

The aromas were analyzed with a Hewlett-Packard (HP) HP5890II capillary GC with a HP 7673A automatic sampler. The column was a 0.5- μm Supelcowax 10 (Supelco, Inc., Bellefonte, PA), 30 m \times 0.32-mm i.d., and the carrier gas H₂ had a 40 cm·s⁻¹ linear velocity. The temperature program was 65 °C for 6 min and then an 8 K·min⁻¹ ramp up to 230 °C for 5 min. The injection volume was 2 μL , and the split ratio was 10 to 1 for the solvent trap samples and 40 to 1 for the liquid-phase samples.

The *n*-alkanes were analyzed with a Hewlett-Packard HP5890 capillary GC with a HP 7671A automatic sampler. The column was a 5.0- μm DB-1 (J&W, Folsom, CA), 30 m \times 0.32-mm i.d., and the carrier gas H₂ had a linear velocity of 40 cm·s⁻¹. The temperature program was 40 °C for 0 min and then a 15 K·min⁻¹ ramp up to 240 °C for 24 min. The injection volume was 2 μL , and the split ratio was 10 to 1 for the solvent trap samples and 40 to 1 for the liquid-phase samples.

Estimation of Equilibrium Partition Coefficients from Activity Coefficients

For dilute concentrations of solute in the gas and liquid phases the mole fractions can be approximated by

Table 2. Table of Uncertainties

Systematic Uncertainties		
	absolute uncertainty	relative uncertainty
gas flow rate		0.001
time (900 min)	2	0.00222
volume 1 (100 cm ³)	0.5 cm ³	0.005
volume 2 (100 cm ³)	0.5 cm ³	0.005
GC area units		0.025–0.050
GC calibration		0.033–0.054
total systematic uncertainty		0.075
Random Uncertainties		
	w_i (ethanol)	range of cv ^a (%)
Solvent Trap $K_{L/G}$		
<i>n</i> -alkanes	1.0	9.7–36
	0.66	8.8–32
	0.33	4.8–43
aromas	1.0	6.7–33
	0.75	9.3–20
	0.50	11–66
	0.35	5.7–36
Concentration Difference $K_{L/G}$		
<i>n</i> -alkanes	1.0	6.5–21
	0.66	13–44
	0.33	2.7–42
Total $K_{L/G}$ Measurement Uncertainties		
solute	w_i (ethanol)	range of cv ^a (%)
Solvent Trap Measurements		
<i>n</i> -alkanes	1.0	12.1–37.8
	0.66	11.4–34.0
	0.33	8.72–44.5
aromas	1.0	9.89–35.0
	0.75	11.8–23.0
	0.50	13.2–67.0
	0.35	9.24–38.1
Concentration Difference Measurements		
<i>n</i> -alkanes	1.0	18.0–24.0
	0.66	15.3–45.6
	0.33	7.76–43.6

^a cv (%) = percent coefficient of variation = 100(sd)/av.

$$y_i^G \approx c_i V_G / M_i \approx c_i^G RT / M_i P \quad (4)$$

$$x_i^L \approx c_i^L V_L / M_i \quad (5)$$

where c_i is the concentration (mass per unit volume), M_i is the solute molecular weight, V is the molar volume of the liquid or gas, R is the gas law constant, T is in kelvin, and P is the total system pressure. The equilibrium concentration partition coefficient, $K_{L/G}$, is defined as the ratio of the concentration (mass per unit volume) of the solute in the liquid (c_i^L) to the concentration (mass per unit volume) of the solute in the gas (c_i^G). Combining eqs 4 and 5 with the definition of the partition coefficient gives

$$K_{L/G} = c_i^L / c_i^G = \Phi_i^L P V_G / (\gamma_i^L V_L P_i^\circ) \quad (6)$$

where Φ is the gas-phase fugacity coefficient. If the behavior in the gas phase is assumed to be nearly ideal, then

$$K_{L/G} = c_i^L / c_i^G = RT / (\gamma_i^L V_L P_i^\circ) \quad (7)$$

It should be noted that the concentration ratio definition of the partition coefficient is the same using either mass or molar concentration ratios.

The original version of UNIFAC (16) using the interactive BASIC program written by Sandler (17) updated with the

Table 3. *n*-Alkanes: Experimental versus Estimated $K_{L/G}$ Data at 25 °Cⁱ

alkane		av ^a	sd ^e	cv ^b	UNIFAC ^h	GCFLORY ^h	alkane		av ^a	sd ^e	cv ^b	UNIFAC ^h	GCFLORY ^h
$w_i(\text{ethanol}) = 1.0$													
pentane	$K_{L/G}$	79	7.6	10	100	61	decane	$K_{L/G}$	17 000	6100	36	9500	9500
	MB % ^c	2.5	1.2	49				MB %	1.9	1.4	75		
	no. ^d	4						no.	9				
hexane	$K_{L/G}$	200	14	7	270	180	dodecane	$K_{L/G}$	120 000	38 000	32	89 000	76 000
	MB %	2.8	2.5	89				MB %	1.6	1.4	89		
	no.	5						no.	7				
heptane	$K_{L/G}$	530	66	12	700	510	tetradecane	$K_{L/G}$	510 000 ^g	140 000	27	610 000	580 000
	MB %	2.8	2.0	71				MB %	2.2	1.4	63		
	no.	6						no.	5				
octane	$K_{L/G}$	1500	170	12	1800	1400	hexadecane	$K_{L/G}$	1 500 000 ^g	840 000	220 000	4 300 000	4 200 000
	MB %	2.6	3.0	120				MB %	3.5	2.7	4.3		
	no.	6						no.	2 ^j				
nonane	$K_{L/G}$	4900	130	3	4900	4000							
	MB %	0.6	0.5	89									
	no.	3											
$w_i(\text{aqueous ethanol}) = 0.66$													
pentane	$K_{L/G}$	9.5	1.2	13	29	4.3	decane	$K_{L/G}$	420	55.0	13	1000	62
	MB %	4	5.5	35				MB %	2.9	2.6	89		
	no.							no.	5				
hexane	$K_{L/G}$	17	2.6	15	60	7.7	dodecane	$K_{L/G}$	2000	180	9	5000	180
	MB %	5.2	4.0	77				MB %	2.7	1.5	55		
	no.	4						no.	6				
heptane	$K_{L/G}$	36	6.0	17	130	14	tetradecane	$K_{L/G}$	7700	2500	32	22 000	540
	MB %	2.2	1.6	70				MB %	10	12	120		
	no.	4						no.	5				
octane	$K_{L/G}$	89 ^f	39.0	44	260	24	hexadecane	$K_{L/G}$	9600 ^g	15 000	3800	96 000	1500
	MB %	14	13	98				MB %	3.2	3.9	2.5		
	no.	8						no.	2 ^j				
nonane	$K_{L/G}$	130 ^f	160	90	550	40							
	MB %	20	7.2	36									
	no.	2 ^j											
$w_i(\text{aqueous ethanol}) = 0.33$													
pentane	$K_{L/G}$	0.24	0.079	33	7.1	0.077	decane	$K_{L/G}$	1.5			54	0.044
	MB %	56	16	28				MB %	17				
	no.	4						no.	1				
hexane	$K_{L/G}$	0.19	0.0093	5	11	0.073	dodecane	$K_{L/G}$	7.5	3.2	43	140	0.038
	MB %	60	12	20				MB %	29	21	73		
	no.	3						no.	6				
heptane	$K_{L/G}$	0.39	0.14	36	17	0.067	tetradecane	$K_{L/G}$	17	5.5	33	340	0.031
	MB %	47	24	52				MB %	30	20	68		
	no.	5						no.	7				
octane	$K_{L/G}$	0.57	0.11	20	26	0.062	hexadecane	$K_{L/G}$	56	19	34	800	0.024
	MB %	48	24	51				MB %	17	14	81		
	no.	4						no.	7				
nonane	$K_{L/G}$	1.2 ^f	0.28	23	40	0.056							
	MB %	56	8.9	16									
	no.	4											

^a av = average value. ^b cv = percent coefficient of variation (100 (sd)/av). ^c MB % = average absolute percent mass balance, deviation from 100%. ^d no. = number of observations. ^e sd = standard deviation. ^f From difference $K_{L/G}$ measurements. ^g Value has high analytical uncertainty. ^h UNIFAC and GCFLORY estimates calculated at experimental concentrations (eq 6). ⁱ Experimental molar fraction concentrations at $w_i(\text{ethanol})$: 1.0, 1×10^{-4} , 0.66, 3.1×10^{-7} to 4×10^{-5} ; 0.33, = 3.1×10^{-7} to 4×10^{-5} . ^j Ranges are given in place of sd and cv.

fifth update set of interaction parameters (18) was used to estimate the activity coefficient of the solutes at $x_i \approx 1 \times 10^{-5}$.

GCFLORY calculations were carried out as described in ref 19 using the POLGEOS FORTRAN program (version March 5, 1991) obtained from the authors. A newer version of GCFLORY which has been optimized solely for solute/polymer systems is not suitable for estimation of VLE behavior of low molecular mass systems like these (20). GCFLORY calculates a weight basis activity coefficient which is converted to a mole fraction basis activity coefficient by multiplication with the ratio of the molecular weight of the solvent to that of the solute.

The saturated partial vapor pressures of the *n*-alkanes at 25 °C were estimated using the correlation of Ambrose and Walton (21). Vapor pressures for the aroma compounds at 25 °C when outside the Antoine equation temperature limits in refs 22 and 23 were estimated by extrapolating data from higher temperatures using the modified Miller equation as described in ref 24.

Fugacity coefficients for the gas phase were calculated using the correlation of Hayden and O'Connell (26). Pure component parameter data were used where available (25–28); otherwise critical temperatures and pressures were estimated using Joback (25). The mean radius of gyration was estimated using the correlation with the parachor. The dipole moments and association and interaction parameters were estimated using those of similar substances.

Error Analysis

The error analysis was conducted using the principles outlined by Taylor (29). A summary of the error analysis is presented in Table 2, listing ranges for the uncertainties.

Results

***n*-Alkanes.** *n*-Alkane $K_{L/G}$ values in ethanol found in Table 3 were compared to regressed $\ln \gamma$ vs $1/T$ estimates from published infinite dilution activity partition coefficient

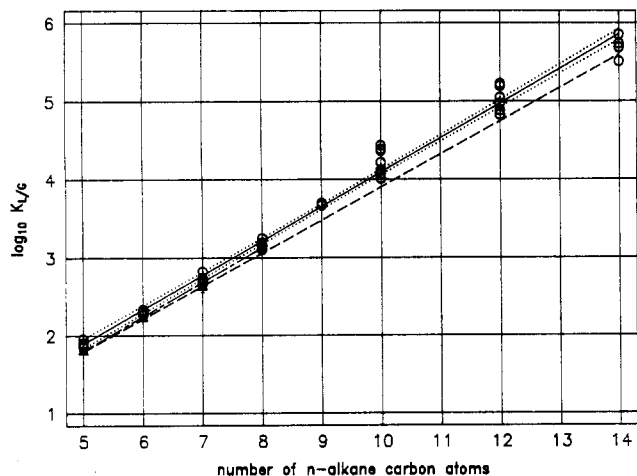


Figure 2. Experimental liquid/gas partition coefficients for *n*-alkanes between ethanol and nitrogen versus literature data at 25 °C: (\blacktriangle) Tieggs et al. (30), (---) PDD (31), (---) experimental regression line confidence bounds, (O) experimental data.

Table 4. Linear Regression Equations $\log K_{L/G}$ vs Number of *n*-Alkane Carbon Atoms (no. of C)

experimental data	$r^2 = 0.988$	$\log K_{L/G} = 0.439(\text{no. of C}) - 0.304$
Tieggs et al.	$r^2 = 1$	$\log K_{L/G} = 0.44(\text{no. of C}) - 0.41$
PDD correlation	$r^2 = 1$	$\log K_{L/G} = 0.42(\text{no. of C}) - 0.32$

data (30) and the experimental data correlation of Pierotti, Derr, and Deal (PDD) (31). The infinite dilution partition coefficients using these activity coefficients were calculated using eq 6. The calculated vapor-phase fugacity coefficients for a vapor-phase concentration of $y_i = 10^{-4}$ ranged from 0.988 to 0.958. Figure 2 compares these $K_{L/G}$ data with published experimental data. The logarithms of partition coefficients of a homologous series of compounds are linear with the molecular weight or in this case the number of carbon atoms (no. of C). The linear regression line equations for the data in Figure 2 are given in Table 4.

At the $\alpha = 0.05$ level of confidence the slope of the experimental data is not significantly different from that of the regressed DECHEMA data line but is significantly larger than that of the PDD correlation. The intercepts of the DECHEMA and PDD correlation are not significantly different from the experimental intercept at the $\alpha = 0.05$ level of significance.

Table 3 summarizes the experimental $K_{L/G}$ for *n*-alkanes in ethanol and aqueous ethanol solutions and compares them to the UNIFAC and GCFLORY estimations. There are several recognizable trends and some limitations of the results that should be pointed out. As the ethanol solution becomes more aqueous $K_{L/G}$ decreases while its variability increases. The increase in scatter can also be seen in the increase in the variation of the absolute mass balance as the liquid phase becomes more aqueous. This is largely due to the analytical problems of injecting aqueous solutions into gas chromatographs using split injection. The large mass balance deviations found with the aqueous solutions can be attributed to sampling and chromatographic errors in the initial liquid-phase concentrations. The $K_{L/G}$ are believed to be correct because values calculated using the liquid-phase concentration difference in eq 3 agree with $K_{L/G}$ values calculated using the solvent traps in eq 1. Some liquid-phase concentration difference $K_{L/G}$ values (eq 3) are included in Table 3 because of GC separation problems between the ethanol and nonane and decane peaks. The peak areas for tetradecane and hexadecane in the pure and $w_i = 0.66$ ethanol solutions were near the GC detection limit; thus, they could contain large

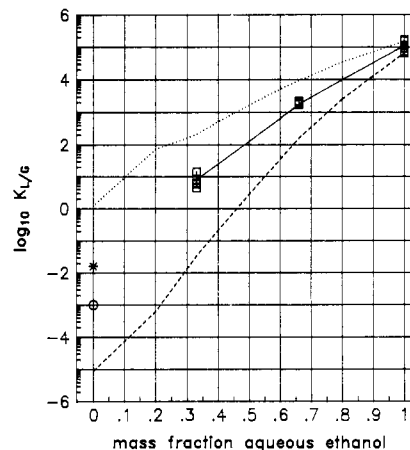


Figure 3. Experimental liquid/gas partition coefficients for dodecane between aqueous ethanol and nitrogen versus UNIFAC- and GCFLORY-estimated partition coefficients at 25 °C: (\ast) PDD (30), (O) Drozd et al. (32), (---) GCFLORY, (---) UNIFAC, (\square) experimental.

systematic errors and should be treated as approximate values.

***n*-Alkanes: Comparison of Estimated with Experimental Results.** Figure 3 is a representative example of how the UNIFAC and GCFLORY partition coefficient estimations for *n*-alkanes vary with ethanol weight fraction. Figure 3 is the dodecane calculated at the experimental mole fractions using eq 6 compared with experimental partition coefficient data. In general, UNIFAC overestimates and GCFLORY underestimates the partition coefficient, with the deviations becoming markedly larger the more aqueous the liquid phase and the larger the *n*-alkane molecule. Neither estimation comes close to the estimation of the correlations for *n*-alkanes in water of Pierotti, Deal, and Derr, (31) and that using an extrapolation of Drozd et al.'s (32) data. The UNIFAC- and GCFLORY-estimated partition coefficients are essentially constant over the experimental concentration ranges used. The effect of the calculated fugacity coefficients on the estimated $K_{L/G}$ values was insignificant, ranging from 0.964 for hexadecane in the vapor phase above ethanol to 0.992 for pentane in the vapor phase above the $w_i = 0.33$ aqueous ethanol solution.

The uncertainty (9–67% of average $K_{L/G}$; see Error Analysis) of the experimental measurements is much smaller than the difference between the model estimates and the experimental means. Neither UNIFAC nor GCFLORY gave good estimations for Drozd et al.'s and Pierotti et al.'s *n*-alkane partition coefficients in water. An average of the UNIFAC and GCFLORY estimations would result in estimations very close to the experimental data.

Aroma Compounds. Table 5 summarizes the measured partition coefficient results for 13 aroma compounds in ethanol and aqueous ethanol solutions and compares them to the UNIFAC and GCFLORY estimations (using eq 6 and the experimental solute concentrations). The experimental aroma measurements behaved similarly to those of the *n*-alkanes in the way the $K_{L/G}$ decreased and the absolute mass balances increased with increasing aqueous content. The literature contains no experimental partition coefficient data to make comparisons with for these compounds. The polar aromas were more difficult to measure than the alkanes because they have a greater affinity for the liquid phase; therefore, the difference in the liquid phase before and after stripping was too small and the $K_{L/G}$ liquid-phase difference method (eq 3) was not used. The alcohols and less volatile aromas such as eugenol and γ -undelacetone were particularly difficult to measure, and their concentrations in the solvent

Table 5. Aroma Compounds: Experimental versus Estimated $K_{L/G}$ Data at 25 °C*

substance		av ^c	sd ^f	cv ^d	UNIFAC ^b	GCFLOWY ^h	substance		av ^c	sd ^f	cv ^d	UNIFAC ^b	GCFLOWY ^h
$w_i(\text{ethanol}) = 1.0$													
isoamyl acetate	$K_{L/G} \times 1000$ MG % ^e no. ^f	13	1.9	14	12	140	dimethylbenzyl-carbinol	$K_{L/G} \times 1000$ MB % no.	640	180	28	1500	2700
D-limonene	$K_{L/G} \times 1000$ MB % no.	16	2.6	16	8.3	0.71	phenylethyl alcohol	$K_{L/G} \times 1000$ MB % no.	670	4.9	1	2300	6700
cis-3-hexenol	$K_{L/G} \times 1000$ MB % no.	140	30	22	220	260	diphenyl-methane	$K_{L/G} \times 100$ MB % no.	530	180	33	430	5400
camphor	$K_{L/G} \times 1000$ MB % no.	150	10	7	170	71	diphenyl oxide	$K_{L/G} \times 1000$ MB % no.	570	160	28	900	830
linalyl acetate	$K_{L/G} \times 1000$ MB % no.	320	46	14	300	350	eugenol ^b	$K_{L/G} \times 1000$ MB % no.	740			31 000	1200
menthol	$K_{L/G} \times 1000$ MB % no.	700	210	29	1500	1600	γ -unde-lactone ^b	$K_{L/G} \times 1000$ MB % no.				9900	9800
citronellol	$K_{L/G} \times 1000$ MB % no.	330	2.4		4100	4600							12 000 ⁱ
$w_i(\text{aqueous ethanol}) = 0.75$													
isoamyl acetate	$K_{L/G} \times 1000$ MB % no.	5.5	0.61	11	8.2	3.9	dimethylbenzyl-carbinol	$K_{L/G} \times 1000$ MB % no.	660			550	340
D-limonene	$K_{L/G} \times 1000$ MB % no.	11	1.0	9	2.7	0.93	phenylethyl alcohol	$K_{L/G} \times 1000$ MB % no.	600			1200	4600
cis-3-hexenol	$K_{L/G} \times 1000$ MB % no.	95	15	16	180	210	diphenyl-methane	$K_{L/G} \times 1000$ MB % no.	240	42	17	58	190
camphor	$K_{L/G} \times 1000$ MB % no.	97	11	11	87	15	diphenyl oxide	$K_{L/G} \times 1000$ MB % no.	240	37	15	340	530
linalyl acetate	$K_{L/G} \times 1000$ MB % no.	130	26	20	160	74	eugenol ^b	$K_{L/G} \times 1000$ MB % no.	640	160	25	350 000	30 000
menthol	$K_{L/G} \times 1000$ MB % no.	670	82	12	540	150	γ -unde-lactone ^b	$K_{L/G} \times 1000$ MB % no.	1100	100	9	3200	1600
citronellol	$K_{L/G} \times 1000$ MB % no.	210	2.8		1800	740			10.2	7.6	74		2400 ⁱ
$w_i(\text{aqueous ethanol}) = 0.50$													
isoamyl acetate	$K_{L/G} \times 1000$ MB % no.	1.2	0.22	19	2.9	0.35	dimethylbenzyl-carbinol	$K_{L/G} \times 1000$ MB % no.	270	61	23	120	29
D-limonene	$K_{L/G} \times 1000$ MB % no.	0.24	0.045	19	0.41	0.092	phenylethyl alcohol	$K_{L/G} \times 1000$ MB % no.	490	320	66	360	1200
cis-3-hexenol	$K_{L/G} \times 1000$ MB % no.	35	4.4	13	79	91	diphenyl-methane	$K_{L/G} \times 1000$ MB % no.	27	3.8	14	5.3	15
camphor	$K_{L/G} \times 1000$ MB % no.	23	2.8	12	23	1.1	diphenyl oxide	$K_{L/G} \times 1000$ MB % no.	25	3.3	14	43	150
linalyl acetate	$K_{L/G} \times 1000$ MB % no.	17	2.8	16	31	8.1	eugenol	$K_{L/G} \times 1000$ MB % no.	810	430	53	70 000	25 000
menthol	$K_{L/G} \times 1000$ MB % no.	120	13	11	110	4.6	γ -unde-lactone	$K_{L/G} \times 1000$ MB % no.	930	820	89	500	39
citronellol	$K_{L/G} \times 1000$ MB % no.	140	19	14	340	36			11	17	160		61 ⁱ
$w_i(\text{aqueous ethanol}) = 0.35$													
isoamyl acetate	$K_{L/G} \times 1000$ MB % no.	0.38	0.022	6	1.3	0.052	dimethylbenzyl-carbinol	$K_{L/G} \times 1000$ MB % no.	95	22	23	34	4.4
D-limonene	$K_{L/G} \times 1000$ MB % no.	35	4.0	12	0.10	0.016	phenylethyl alcohol	$K_{L/G} \times 1000$ MB % no.	200	74	36	140	380
cis-3-hexenol	$K_{L/G} \times 1000$ MB % no.	13	0.83	7	37	44	diphenyl-methane	$K_{L/G} \times 1000$ MB % no.	4.2	0.43	10	0.97	2.6
camphor	$K_{L/G} \times 1000$ MB % no.	6.0	0.42	7	7.6	0.18	diphenyl oxide	$K_{L/G} \times 1000$ MB % no.	3.5	0.38	11	9.2	57

Table 5 (Continued)

substance		av ^c	sd ^e	cv ^d	UNIFAC ^h	GCFLORY ^h	substance		av ^c	sd ^e	cv ^d	UNIFAC ^h	GCFLORY ^h
$w_i(\text{aqueous ethanol}) = 0.35$													
linalyl acetate	$K_{L/G} \times 1000$	2.3	0.16	7	8.4	1.3	eugenol	$K_{L/G} \times 1000$	250	3.7	2	16 500	18 000
	MB %	10	6.6	65				MB %	5.2	2.8	55		
	no.	3						no.	3				
menthol	$K_{L/G} \times 1000$	22	1.4	6	29	0.39	γ -undelactone	$K_{L/G} \times 1000$	310	63	20	120	2.3
	MB %	7.7	7.6	99		0.059 ⁱ		MB %	6.0	3.9	65		3.7 ⁱ
	no.	4						no.	3				
citronellol	$K_{L/G} \times 1000$	73	21	29	90	4.2							
	MB %	3.9	1.7	43									
	no.	3											

^a Aroma compounds listed in GC elution order. Experimental concentration $x_i = 7.7 \times 10^{-6}$. Total solute mole fraction 1×10^{-4} . ^b Results highly uncertain, large error likely. ^c av = average value. ^d cv = percent coefficient of variation (100(sd)/av). ^e MB % = average absolute percent mass balance, absolute deviation from 100%. ^f no. = number of observations. ^g sd = standard deviation. ^h UNIFAC and GCFLORY estimates calculated using experimental mole fractions in liquid and gas phases. ⁱ Estimated using cyclic CH₂ group-contribution parameters.

Table 6. Average Absolute Deviations of Estimation from Experimental $K_{L/G}$ for 13 Aroma Compounds

	$w_i(\text{ethanol}) = 1.0$		$w_i(\text{ethanol}) = 0.75$		$w_i(\text{ethanol}) = 0.50$		$w_i(\text{ethanol}) = 0.35$	
	UNIFAC	GCFLORY	UNIFAC	GCFLORY	UNIFAC	GCFLORY	UNIFAC	GCFLORY
av	490	410	4300	470	720	350	620	750
av (no eugenol)	170	400	120	130	73	130	110	220
av using cyclic groups (no eugenol)		690		130		130		220

trap were often very near the GC detection limit. The effects of lower aroma volatility and their greater affinity for the alcohol phase can be seen in the increasing coefficients of variation for these compounds compared to the *n*-alkanes which had much larger $K_{L/G}$ values.

Aroma Compounds: Comparison of Estimated with Experimental Results. Table 5 compares the UNIFAC and GCFLORY $K_{L/G}$ estimations using eq 6 with experimental measurements for the 13 aroma compounds measured in ethanol and aqueous ethanol solvents. The effect of the estimated fugacity coefficients using the Hayden and O'Connell correlation was minimal for all 13 aroma compounds in the ethanol-water-nitrogen vapor-phase mixtures, ranging between 0.963 and 0.983 depending on the aroma and the percent ethanol. The model $K_{L/G}$ estimates vary very little, decreasing only 5% depending on the solute, over the experimental solute mole fraction range from 1×10^{-7} to 1×10^{-4} . In general, the models estimated hydrocarbon $K_{L/G}$ the best followed by the acetates, with some good estimations for the alcohols.

The uncertainties of some of the vapor pressures at 25 °C used in eq 6 could be as high as 50% depending on how the vapor pressures were estimated. In particular, the vapor pressures for *cis*-3-hexenol, dimethylbenzylcarbinol, diphenyl oxide, and γ -undelactone have some of the largest probable errors since they are estimated using similar substances. The systematic uncertainty of the experimental measurements is approximately $\pm 7.5\%$ of the average, and the total uncertainty ranges from $\pm 9\%$ to $\pm 67\%$ depending on the aroma and the liquid phase (see Error Analysis).

GCFLORY has both cyclic and aliphatic methyl groups, and calculations were made using both of these groups for the cyclic aroma molecules. In general, the calculations using the cyclic groups (c) showed a marked improvement over the aliphatic (a) results with the exception of methanol. In UNIFAC the best fit to the experimental diphenyl oxide data was obtained when the secondary ether group for the ether group contribution and then the one less aromatic carbon group contribution were used (e.g., 10 aromatic CH's, 1 aromatic C, and 1 CHO). Eugenol is an example of a molecule containing multiple functional groups that challenges the group-contribution additive assumptions in both models. The eugenol molecule with its two functional groups, aromatic ring, and unsaturation has some steric hindrance so that the behavior of the functional groups is different from that if

they were part of a mono-functional-group aliphatic molecule. Comparison with eugenol experimental data, which have large experimental variation, nevertheless shows there may be large deviations between the model's estimation and experiment.

Table 6 summarizes the average absolute deviations (AAD) for the UNIFAC and GCFLORY aroma compound estimations from the experimental $K_{L/G}$ data for the 13 aroma compounds in aqueous ethanol solutions.

The average absolute deviations in Table 6 show the GCFLORY estimates for all 13 aroma compounds to be better than the UNIFAC estimates except for the $w_i = 0.35$ aqueous ethanol solution. However, when the worst estimated solute for both models, eugenol, is removed from the average, UNIFAC has a better AAD for the 12 remaining compounds. The third set of averages shows that the GCFLORY cyclic group contributions are on average the same or worse than those of the aliphatic groups.

Discussion

The $K_{L/G}$ measurements show that the gas stripping column method can give results comparable to those from other liquid/gas partition coefficient measurement methods and allows measurements using very dilute solute concentrations to be made. The results also show that mixtures of solutes in dilute solutions can be used in this method without significant interaction effects on the measured partition coefficients relative to the measurement uncertainties. This significantly reduces the work needed to measure a series of solutes. Gas and liquid flows must be optimized depending on the partition coefficients of the solutes being measured. The partition of solutes between the liquid and gas phases is determined mainly by the vapor pressure of the substance and activity coefficient (which is related to its solubility) in the liquid phase. It is therefore advisable to select a series of solutes for use in a mixture which have similar vapor pressures and solubilities in the liquid phase (while still remaining compatible with the analytical method, i.e., separable with GC). Solutes with widely varying partition coefficients cause analytical problems when one substance is minimally found in the gas trap (large $K_{L/G}$) while the other has saturated the solvent in the trap after a given measurement time period (small $K_{L/G}$). Concentration effects on the $K_{L/G}$ appear to be negligible compared to the uncertainties of the measurements in dilute concentrations with mole fractions of less than 1×10^{-4} .

When very exact determinations of $K_{P/L}$ values are needed, the UNIFAC and GCFLORY estimation methods may not be accurate enough for all substances. However, considering that these two methods estimated partition coefficients over 5 orders of magnitude ($10 < K_{L/G} < 1\,000\,000$) using nothing other than the molecular structures of the system's components in the form of group-contribution parameters, it is a remarkable achievement. Furthermore, it is remarkable that the GCFLORY model which was developed for polymer mixtures estimates activity coefficients for low molecular weight mixtures as well as it does. Both models can successfully reflect the natures of the different solutes in their estimations. As might be expected the vapor-phase fugacity correction (itself estimated) had little effect at the measurement conditions of atmospheric pressure and 25 °C, and therefore, the assumption of ideal gas behavior in eq 7 can be used without significant loss of estimation accuracy. The UNIFAC and GCFLORY estimation methods could be successfully used for estimating partition coefficients for use in food/package systems provided the user has an idea of the expected order of magnitude of the partition coefficients in the system so that outlier estimations can be rejected. There are other versions of UNIFAC (33–35), other group-contribution methods (36), or other equation of state methods (37) which may be more accurate than the UNIFAC and GCFLORY methods evaluated here.

The users of these estimation methods should critically examine their estimations and be aware of the potential for significant variation from experimental data. It is suggested that the users of these methods compare the order of magnitude of these estimations to those of experimental data for similar systems by making intuitive comparisons of the magnitudes of the estimated partition coefficients for solutes with different polarities.

Conclusions

Measurements of liquid/gas partition coefficients for *n*-alkanes (octane to tetradecane) and 13 aroma compounds partitioned between ethanol and aqueous ethanol solutions and nitrogen have been made in the infinite dilution concentration range. This is the first time partition data over a range of ethanol and aqueous ethanol concentrations have been measured for these substances. The equilibrium stripping column method is useful for measuring partition coefficients of substances with low volatilities in relatively volatile solvent mixtures.

With respect to their current levels of development and with respect to their ability to quantitatively estimate solute partition coefficients between gas and ethanol and aqueous ethanol solutions, UNIFAC is better than GCFLORY in several aspects. UNIFAC is applicable to a wider range of solutes and on average predicted their liquid/gas partition coefficients better. UNIFAC also had fewer estimations having greater than an order of magnitude error for the estimations of the solutes tested. UNIFAC can estimate aqueous ethanol liquid activity coefficients better than GCFLORY which had large deviations the more aqueous the solution became. Both are comparable for ease of use. Both methods had particular problems with ring structures and multi-functional-group solutes. There are no user inputs into these two models. In general, with UNIFAC the simpler the solute structure, the better chance of a good partition coefficient estimation. GCFLORY showed no systematic variation in its ability to estimate different molecular structures.

Literature Cited

- Baner, A. L.; Bieber, W.; Figge, K.; Franz, R.; Piringer, O. *Food Addit. Contam.* **1992**, *9*, 137.
- Recommendation for Chemistry Data for Indirect Food Additive Petitions*, Version 1.1; Division of Food Chemistry & Technology, Center for Food Safety & Applied Nutrition, Food & Drug Administration, Department of Health and Human Services: Washington, DC, 1988.
- Off. J. Eur. Communities* **1985**, L372, 14.
- Olson, J. D. *Fluid Phase Equilib.* **1989**, *52*, 209.
- Dohnal, V.; Horáková, I. *Fluid Phase Equilib.* **1991**, *68*, 173.
- Hussam, A.; Carr, P. W. *Anal. Chem.* **1985**, *57*, 793.
- Hradetzky, G.; Wobst, M.; Vopel, H.; Bittrich, H.-J. *Fluid Phase Equilib.* **1990**, *54*, 133.
- Turek, E.; Arnold, D.; Greenkorn, R. A.; Chao, K. *Ind. Eng. Chem. Fundam.* **1979**, *18*, 426.
- Landau, I.; Belfer, A. J.; Locke, D. C. *Ind. Eng. Chem. Res.* **1991**, *30*, 1900.
- Mackay, D.; Shiu, W. Y.; Sutherland, R. P. *Environ. Sci. Technol.* **1979**, *13*, 333.
- Murphy, T. J.; Mullin, M. D.; Meyer, J. A. *Environ. Sci. Technol.* **1987**, *22*, 155.
- Kolb, B.; Welter, C.; Bichler, C. *Chromatographie* **1992**, *34* (5–8), 235.
- Ettre, L. S.; Welter, C.; Kolb, B. *Chromatographie* **1993**, *35* (1/2), 73.
- Piringer, O.; Sköries, H. In *Analysis of Volatiles*; Schreider, P., Ed.; Walter de Gruyter & Co.: Berlin, 1984; p 49.
- Brunner, S.; Hornung, E.; Santl, H.; Wolff, E.; Piringer, O. G.; Altschuh, J.; Brüggermann, R. *Environ. Sci. Technol.* **1990**, *24*, 1751.
- Fredenslund, A.; Gmehling, J.; Rasmussen, P. *Vapor-liquid Equilibria using UNIFAC*; Elsevier: Amsterdam, 1977; p 103.
- Sandler, S. I. *Chemical and Engineering Thermodynamics*; John Wiley and Sons: New York, 1989.
- Hansen, H. K.; Rasmussen, P.; Fredenslund, A.; Schiller, M.; Gmehling, J. *Ind. Eng. Chem. Res.* **1991**, *30*, 2352.
- Chen, F.; Fredenslund, A.; Rasmussen, P. *Ind. Eng. Chem. Res.* **1990**, *29*, 875.
- Bogdanic, G. IVC-SEP Phase Equilibria and Separation Processes. MAN 9305, Manual GC-FLORY; Institut for Kemiteknik: Lyngby, Denmark, May 1993.
- Ambrose, D.; Walton, J. *Pure Appl. Chem.* **1989**, *61*, 1395.
- Boublik, T.; Fried, V.; Hala, E. *The Vapor Pressures of Pure Substances*; Elsevier: Amsterdam, 1973.
- Perry, R. H.; Green, D. W.; Maloney, J. O. *Perry's Chemical Handbook*; McGraw-Hill: New York, 1984.
- Bertucco, A.; Piccinno, R.; Soave, G. *Chem. Eng. Commun.* **1991**, *106*, 177.
- Reid, R. C.; Prausnitz, J. M.; Poling, B. E. *The Properties of Gases and Liquids*; McGraw-Hill: New York, 1986.
- Prausnitz, J. M.; Anderson, T. F.; Grens, E. A.; Eckert, C. A.; Hsieh, R.; O'Connell, J. P. *Computer Calculations for Multicomponent Vapor-Liquid and Liquid-Liquid Equilibria*; Prentice-Hall, Inc.: Englewood Cliffs, NJ, 1980.
- McClellan, A. L. *Tables of Experimental Dipole Moments*; W. H. Freeman: San Francisco, 1963.
- McClellan, A. L. *Tables of Experimental Dipole Moments*; Raha Enterprises: El Cerrito, CA, 1974; Vol 2.
- Taylor, J. R. *An Introduction to Error Analysis*; University Science Books: Mill Valley, CA, 1982.
- Tiegs, D.; Gmehling, J.; Medina, A.; Soares, M.; Bastos, J.; Alessi, P.; Kikic, I. *Activity Coefficients at Infinite Dilution*; DECHEMA Chemistry Data Series; DECHEMA: Frankfurt, 1986; Vol. IX, Part I.
- Pierotti, G. J.; Deal, C. H.; Derr, E. L. *Ind. Eng. Chem.* **1959**, *51*, 95.
- Drozd, J.; Vejrosta, J.; Novak, J.; Jönsson, J. A. *J. Chromatogr.* **1982**, *245*, 185.
- Bastos, J. C.; Soares, M. E.; Medina, A. G. *Ind. Eng. Chem. Res.* **1988**, *27*, 1269.
- Larsen, B. L.; Rasmussen, P.; Fredenslund, A. *Ind. Eng. Chem. Res.* **1987**, *26*, 2274.
- Weidlich, U.; Gmehling, J. *Ind. Eng. Chem. Res.* **1987**, *26*, 1371.
- Kojima, K.; Tochigi, K. *Prediction of Vapor Liquid Equilibrium by the ASOG Method*; Elsevier: Amsterdam, 1979.
- Anderko, A. *Fluid Phase Equilib.* **1990**, *61*, 145.

Received for review August 4, 1993. Revised November 1, 1993. Accepted November 19, 1993.* The authors would like to thank the Deutsches Bundesministerium für Ernährung, Landwirtschaft und Forsten for their support.

* Abstract published in *Advance ACS Abstracts*, February 15, 1994.